LAWRENCE
LIVERMORE
NATIONAL
LABORATORY

LLNL-TR-827450

Fission-product decay studies with the FRIB Decay Station

K. Kolos, D. E. M. Hoff, N. D. Scielzo

October 4, 2021

Disclaimer

This work performed under the auspices of the U.S. Department of Energy by Lawrence Livermore National Laboratory under Contract DE-AC52-07NA27344.

Full technical report

Fission-product decay studies with the FRIB Decay Station

K. Kolos (kolos1), D. E. M. Hoff (hoff8), N. D. Scielzo (scielzo1)

FS-LDRD-011

Abstract

The Facility for Rare Isotopes Beams (FRIB) will be the flagship facility in low-energy nuclear physics when it comes online in 2022. This U.S. Department of Energy Office of Science user facility will open-up a multitude of new opportunities to study exotic nuclei and will lead to new discoveries in nuclear structure, nuclear astrophysics, fundamental symmetries, and isotopes of importance to nuclear applications. The β-decay properties of neutron-rich isotopes will be measured with the FRIB Decay Station, a sophisticated state-of-the-art modular multi-detector system envisioned to perform β, γ, n, and charged-particle spectroscopy. In this feasibility study, we use nuclear decay data collected with the FRIB Decay Station precursor, the Beta-Counting Station, currently used at Michigan State University with a radioactive beam produced at the National Superconducting Cyclotron Laboratory to identify the FRIB Decay Station capabilities for future measurements of neutron-rich exotic nuclei at FRIB to help provide a path forward for future measurements of interest to the lab's mission.

Background and Research Objectives

The emerging Facility for Rare Isotopes Beams (FRIB) will deliver a broad range of primary beams from hydrogen to uranium that will be used for the in-flight production of rare exotic nuclei. With this unprecedented access to exotic beams FRIB is estimated to double the number of known isotopes from what is currently known. The FRIB Decay Station (FDS) [1] will be uniquely positioned to make crucial contributions towards discovery experiments at the extremes of the accessible regions and will have a transformative impact on our understanding of nuclear structure, nuclear astrophysics, fundamental symmetries, and isotopes of importance to applications. FDS goals are well aligned with the priorities and overarching science goals that have been formulated by the broader nuclear science community, most recently in the 2015 NSAC Long Range Plan [2].

The FDS is a sophisticated versatile multi-detector array that will be composed of a large volume High-Purity Germanium (HPGe) detector array, LaBr detector array, an implantation detector (SiDSSD, $CeBr_3$, GeDSSD, XScint), a neutron detector "NEXT", and a total absorption spectrometer (MTAS, SuN). This novel approach of multi-detector-array will enable execution of multiple measurements in succession or in one experiment to take advantage of a multi-isotope fragmentation beam that will be delivered from FRIB. The exact configuration of the detector arrays will be dependent on the specific science goals of each experiment and involve tradeoffs between energy resolution, time resolution, efficiency, and background. Each experiment is predicted to acquire data on close to 10-20 isotopes in the same mass region. The FDS will allow measurements of multiple decay properties of these exotic nuclei at the same time to maximize the scientific opportunity and impact of each experiment.

The LLNL team have already established prominent roles in the FDS working group, which is comprised of over 100 scientists from 26 institutions in the United States. K. Kolos is an elected member of the FDS Users Executive Committee and N. D. Scielzo is a convener for the FDS working group. Close to 10 detectors of the HPGe array of the FDS will be LLNL-owned (J. Harke). The effort described in this report, was the first step for establishing a larger LLNL decay spectroscopy program at FRIB through realizing data analysis challenges and capabilities related to the FDS.

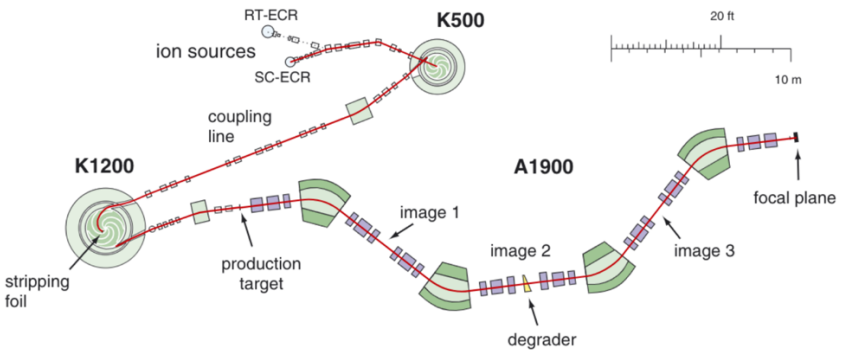

Figure 1: A schematic diagram of the coupled cyclotrons and A1900 fragment separator at the NSCL from Ref. [3].

Scientific Approach and Accomplishments

An assessment of the capabilities and challenges associated with the FDS were accomplished by analyzing existing data from an experiment performed recently at Michigan State University (MSU) and National Superconducting Cyclotron Laboratory's (NSCL) with the precursor of the FRIB Decay Station, the Beta-Counting Station (BCS).

Experimental details

The radioactive ions were produced with a primary 140 MeV/nucleon beam of ^{86}Kr beam accelerated through the coupled K500 and K1200 cyclotrons shown in Fig. 1. The primary beam impinges on a 320 mg/cm^2 ^{9}Be target fragmentation target, and the fragments are then passed through the A1900 fragment separator [3] selecting for the ions of interest before arriving to the detection system. The multi-detector array used in this experiment had similar characteristics to a typical FDS configuration, and most of these detectors will be incorporated in the FDS for the initial measurement campaigns at FRIB. The fragmentation beam was implanted on the $CeBr_3$ detector (dimensions 51 mm x 51 mm x 3 mm) coupled to a pixelated photomultiplier tube (16x16 pixels). The pixilation provided by the photomultiplier tube allows for a greater characterization of the implanted activity greatly reducing the overall background. The implantation detector was surrounded by 16 HPGe clover detectors to measure the subsequent gamma-ray radiation. Furthermore, 16 LaBr detectors were used to measure the short lifetimes of decays via gamma-ray emission, as these are known to have very good timing properties. Three Si PIN detectors, two upstream and one downstream of the $CeBr_3$ detector, were used for vetoing light ions and particle identification. This was performed by energy loss measurements in one of the upstream Si PIN coupled with time-of-flight (TOF) information of the ion from a scintillator at the focal plane of the A1900 fragment separator. This method gives rise a particle-identification (PID) plot, see Fig. 2, with the isotopes implanted onto the $CeBr_3$ detector. The subsequent decay information of multiple isotopes (e.g., $^{75\text{-}77}$Cu, $^{77\text{-}79}$Zn, $^{79\text{-}81}$Ga and $^{82\text{-}84}$Ge) were measured through a series of correlating events in HPGe and LaBr detectors with these implants. For the data acquisition (DAQ), all the signals were fed into XIA [4] Pixie-16 modules and energy, timing, and in the case of the $CeBr_3$ detector trace information were stored.

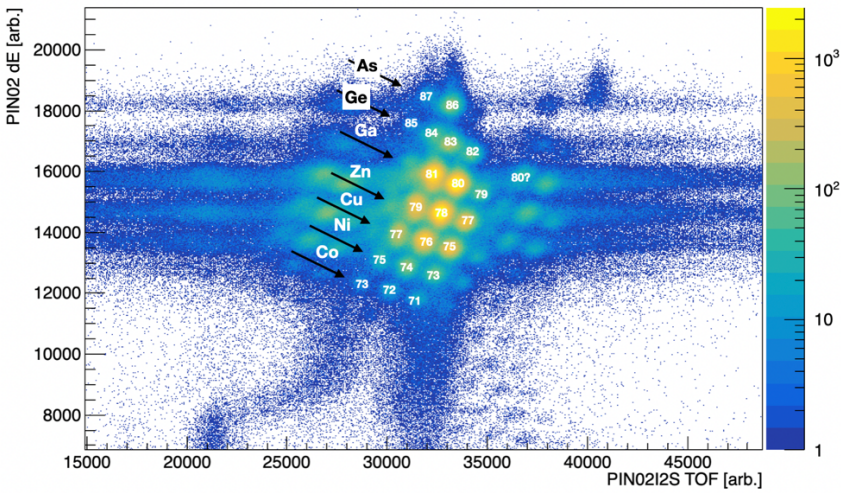

Figure 2: A PID plot from the experiment at the NSCL showing the different isotopes implanted into the CeBr detector. The y-axis shows the energy-loss detected in the second Si PIN while the x-axis shows the TOF to the detector system.

HPCC

The analysis of the events was performed at the High-Performance Computing Center (HPCC) at Michigan State University (MSU). This experiment was one of the first to utilize the HPCC for offline analysis. The HPCC at MSU allows for outside collaborators to make an account at the request of an on-site collaborator. The analysis software can then also be version-controlled through the MSU Gitlab and modified for future experiments. The analysis for this experiment is pioneering the use of high-performance computing that will be necessary for future FRIB experiments.

LLNL-developed correlation code

The correlation algorithm we developed for this study works as follows:

1. Events in the $CeBr_3$ are identified as either **implants** or **decays**. Implants are differentiated by checking that the two Si PIN's at the front of the detector system fired in coincidence (20 us) with the $CeBr_3$ detector. Decays are in anticoincidence.
2. If the event is an **implant** event, then the most likely implant pixel is determined by fitting the spatial signal distribution found in the photomultiplier tube coupled to the $CeBr_3$ detector. The implant is then saved to a list of ions implanted into that pixel within a correlation-time window.
3. If the event is determined to be a **decay** event, a most likely pixel is found in the same manner as an implant event. A list of correlated implant events is then generated by looking through the lists of ions within a user-defined tolerance (1x1 – 5x5 pixels) centered on the identified pixel.
4. The information for each of these events along with the coincident gamma-ray detector events create an event that is later analyzed.

The list of generated decay events can then be further processed, providing correlation times between implants and decays as well as the associated gamma-ray decays. By gating on a particular ion in the PID, correlations between decay events are found within a particular correlation window. If the decay is truly associated with a particular implant, then it will follow an exponential-decay distribution in time with the implant. In order to find the correlation signal background, the analysis can be run in "reverse" where the time-ordered list of events is sorted from greatest to least time, thereby removing any true coincidences in the resulting spectra. A schematic of the analysis process is shown in Fig. 3, where the "forward"

direction correlates decays with implants occurring before, and the "reverse" correlates decays with implants later in time. For the presented analysis, a correlation window of 30 s and a tolerance 3x3 pixels was used.

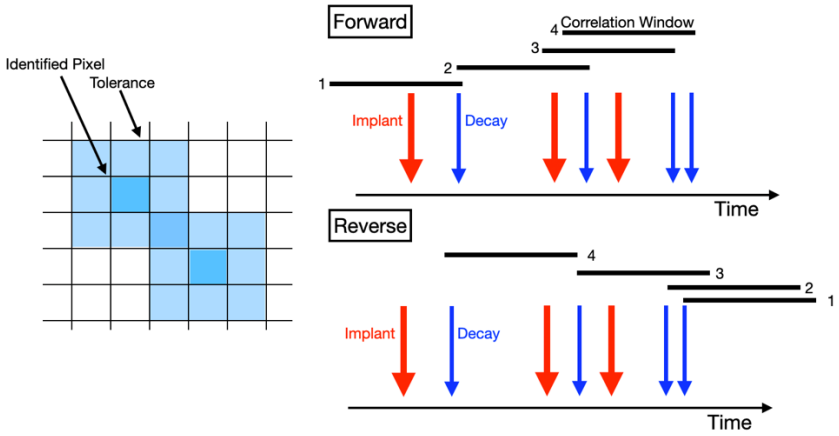

Figure 3: A schematic of the analysis process. As implants are detected they are stored in a list for each identified pixel up to a specified correlation-time window. When a decay signal is found implants are searched within a tolerance of the identified decay pixel. As the figure on the right shows, a given decay can be associated with multiple implants, but only true decays will be correlated in time with the implant event. The analysis can be run in "reverse" where the list is run in time-reversed order. This guarantees that the decay events will be uncorrelated providing a measure of the uncorrelated background in the experiment.

Half-lives and intensity determination

For this analysis, the time-correlated spectra that were found in the reverse sorting were used as a background for the forward spectra. An example of the resulting background subtracted time-correlation spectrum as well as the correlated gamma rays are shown for the case of ^{80}Ga implants in Fig. 4.

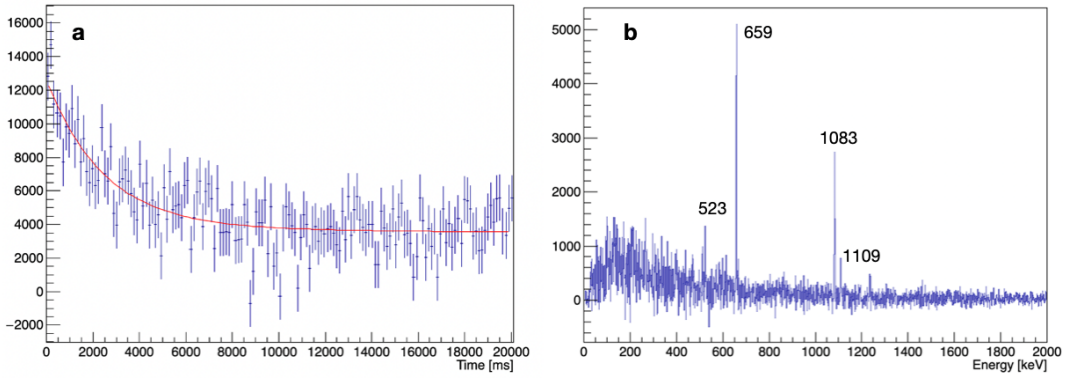

*Figure 4: (**a**) A plot of decay events correlated in time with ^{80}Ga implants. The spectrum has been background subtracted with the reverse-sorted time spectrum. (**b**) A plot of the gamma rays associated with the decay events within 10 s of ^{80}Ga implantation background subtracted with the reverse-sorted time spectrum.*

The measured activity above the randomly-correlated background show in in Fig. 4(a) will include contributions from daughter and granddaughter decays. Therefore, to extract the correlation signal the half-lives for the daughters and granddaughters were fixed to the values from NNDC and fed into the resulting solution of the Bateman equations for a full characterization of the resulting activity. From the

fit shown by the solid red-line in Fig. 4(a), the half-life of the parent can be found, as well as the total number of parent decays detected which can be used to determine branching ratios.

An example of the time-correlations of gamma-rays is shown in Fig. 5, which shows the time correlation of decays after ^{76}Cu implants, as well as some of the correlated gamma-rays. The case of ^{76}Cu shows the utility of looking at these time correlation spectra with gamma-rays. The gamma-ray spectra collected 5s after ^{76}Cu implants shows a peak at 199 keV, however this line is not correlated in time with the ^{76}Cu implant time. This is the most intense gamma ray in the decay of the daughter ^{76}Zn, so it is expected to be seen shortly after implants of ^{76}Cu.

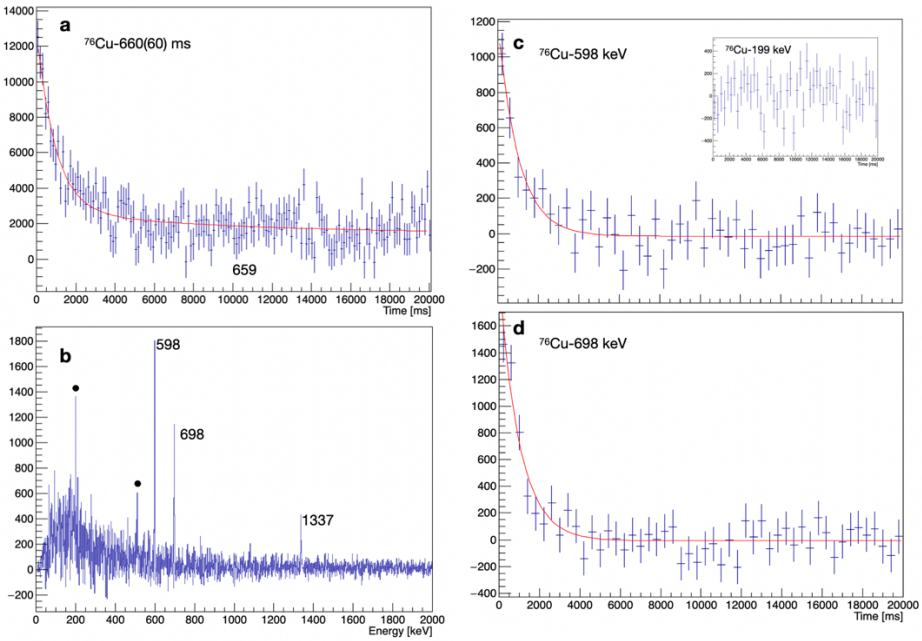

*Figure 5: (**a**) The background-subtracted time-correlation of decay events after ^{76}Cu implants. (**b**) The background-subtracted gamma-rays observed within 5 s of ^{76}Cu implants. The labeled gamma-rays come from de-excitation in the daughter ^{76}Zn. The circle transitions come from other processes. (**c**) 598-keV gamma rays and (**d**) 698-keV gamma rays with ^{76}Cu implants also subtracted by the same spectra found in reverse correlation. The solid red-lines show a fit with an exponential and constant background. The inset shows the results of an uncorrelated gamma ray that appears in the beta-gated gamma-ray spectrum, in this case for 199-keV peak found after ^{76}Cu implants which is due to the daughter ^{76}Zn decays.*

Table 1 shows a list of the half-lives that were determined with the correlation analysis, along with gamma-rays that were measured above background.

Table 1: A list of all of the halflives and measured gamma rays for each of the isotopes with reasonable statistics observed in the PID. Good agreement is found for the literature halflives . By looking at the gamma-ray correlations the transition can be confirmed to come from the implanted nucleus.

Isotope (N_{ions})	Half-life NNDC (ms)	Half-life measured (ms)	Gamma-rays measured (keV)	Half-life from correlated gamma-rays (ms)
^{73}Ni (53,000)	842(30)	640(160)	—	—
^{74}Ni (74,000)	507.7(46)	440(60)	—	—

^{75}Cu (310,000)	1224(3)	1060(170)	—	—
^{76}Cu (360,000)	638(9)	660(60)	199	No Corr. (^{76}Zn)
			598	700^{800}_{630}
			698	710^{900}_{590}
			1337	460^{640}_{360}
^{77}Cu (160,000)	468.1(20)	420(50)	—	—
^{77}Zn (250,000)	2080(50)	1900(270)	—	—
^{78}Zn (1,050,000)	1470(150)	1180(60)	182	970^{1530}_{705}
			224	965^{1530}_{700}
			281	1000^{2100}_{700}
			454	1700^{2300}_{1400}
			619	No Corr. (^{78}Ga)
			635	1170^{2100}_{815}
			860	1700^{3100}_{1200}
			979	1500^{3300}_{1000}
^{79}Zn (160,000)	756(42)	660(130)	—	—
^{79}Ga (37,000)	2847(3)	2200(1300)	—	—
^{80}Ga (950,000)	1676(14)	1790(230)	525	1000^{8000}_{500}
			659	2100^{2500}_{1800}
			1083	1420^{1690}_{1220}
			1109	1620^{2080}_{1330}
^{81}Ga (800,000)	1217(5)	1100(120)	—	—

The largest source of error in these types of experiments comes from the improper correlation of decays after an implant event. In the case that only one species is being implanted then the largest half-life that one can measure with statistics being the limiting factor is given by $\tau_{1/2,best} = \ln(2)/R$, where R is the

implantation rate of the species into a given detector. The pixelization of the implantation detector allows each pixel (or group of pixels) to be treated as separate detectors, thereby reducing this factor, and allowing for longer correlation times. In a typical experiment there will be multiple species being implanted, which complicates a prescription for determining the largest half-life that can be measured well, and the overall beam distribution of ions also changes the rate into a given pixel. In the experiment outlined here, the implantation rate per pixel was about 2Hz giving a $\tau_{1/2,best} = 350$ ms. This estimate ignores the spatial distribution of implants, and thus in reality this number will be much lower. As can be seen in Table 1, for the shorter-lived species, the half-lives can be determined with uncertainties of ~1%, even when these had significantly lower total implantation. In fact, the uncertainty on the half-life for ^{78}Zn was improved by a factor of 3.

To extract gamma-ray intensities of the decaying isotopes, the fit to the time-correlation plots show in in Figs. 4(a) and 5(a) can be used to extract the total number of decays detected based on the total measured activity. After obtaining the efficiencies for detecting a particular transition, whether experimentally or with a simulation, the resulting branching ratios can be calculated.

Results for an isomer: ^{76}Zn-to-^{76}Cu decay

Another important advantage of this experiment is recording traces for sygnals in $CeBr_3$ detector, which allowed us for isomer studies and measurements of half-lives and gamma rays from subsequent decays. In the even of internal-conversion following beta decay event, the ejected electron will leave another signal in the active implant detector resulting in two traces (opposed to one if it was only a decay event). By analyzing these double-pulse events, short-lived isomer in ^{76}Zn was found following the beta-decay of ^{76}Cu. This approach as well as results are detailed in Ref. [5] which was recently submitted for publication. Our correlation algorithm improved the statistics of correlated gamma-rays from ^{76}Cu decays by a factor of 4 compared to the original algorithm, which only correlated decay events with the most recent implant event.

Outlook and improvements

When looking towards future experiments at FRIB, one of the main concerns is the built-in activity of implanted ions coupled with the rate of implantation, which is expected to be significantly higher with FRIB. For performing correlations, the inverse implantation rate per pixel of the detector is the main consideration. A highly segmented detector, along with sweeping the beam across the detector, would help reduce the rate on any-one pixel; for example, by replacing the $CeBr_3$ with a 40x40 Si detector and sweeping the beam the experiment could achieve a $\tau_{1/2,best} = 2.2$ s. More careful planning would be required to ensure implantation into the Si detector when using the higher energy beams that will be delivered by FRIB. The configuration of the implantation detector should therefore be selected based on the main goal of the experiment.

Mission impact

The FRIB Decay station will provide a new and unique capability enabling access to numerous radioisotopes in unprecedented quantities and at higher purities than previously available. With this system, decay data on short-lived neutron and proton-rich isotopes as well as their decaying isobars will be available for high-priority measurements of interest to the community and to the Lab. As a result, measurements of decay properties such as half-lives or gamma-ray transition intensities of radioisotopes important to national security needs will be feasible in the coming years. Generating a shortlist of priority measurements important to national security needs is the next priority.

Conclusion

We have performed a study identifying the capabilities and limitations of a sophisticated decay array at FRIB. We have demonstrated that half-lives and other properties can be reliably extracted, including the half-life of implanted ions and even the half-life of particular excited states [5]. Improvements to the experimental setup for the purpose of measuring branching ratios has been suggested, and primarily rely on the choice of implantation detector used. Overall, these results will be used to guide future research plans and funding opportunities both internally at LLNL and externally via funding opportunities that arise from the DOE/SC and NNSA.

References

[1] FRIB Decay Working Group, "The FRIB Decay Station," [Online]. Available: https://indico.frib.msu.edu/event/2/attachments/57/209/FRIB_Decay_Station_WP.pdf.

[2] The Nuclear Science Advisory Comittee, "Reaching for the Horizon: The 2015 Long Range Plan for Nuclear Science," 2015.

[3] A. Stolz, T. Baumann, T. Ginter, D. Morissey, M. Portillo, B. Sherrill, M. Steiner and J. Stetson, "Production of Rare Isotope Beams with the NSCL Fragment Separator," *NIM B,* vol. 241, pp. 858-8561, 2005.

[4] C. J. Prokop, S. N. Liddick, B. L. Abromeit, A. T. Chemey, N. R. Larson, S. Suchyta and J. R. Tompkins, "Digital data acquisition system implementation at the National Superconducting Cyclotron Laboratory," *NIM A,* vol. 741, pp. 163-168, 2014.

[5] A. Chester, B. A. Brown, S. P. Burcher, M. P. Carpenter, J. J. Carroll, C. J. Chiara, P. A. Copp, B. P. Crider, J. T. Harke, D. E. M. Hoff, K. Kolos, S. N. Liddick, B. Longfellow, M. J. Mogannam, T. H. Ogunbeku, C. J. Prokop, D. Rhodes and R, "Identification of a new isomeric state in 76Zn following the beta-decay of 76Cu," *(Under Review at Physical Review C),* 2021.

Publications, presentations

A. Chester et. al. “Identification of a new isomeric state in ^{76}Zn following beta-decay of ^{76}Cu” submitted for publication to PRC, LLNL-JRNL-823738

Abbreviated report

Fission-product decay studies with the FRIB Decay Station

K. Kolos (kolos1), D. E. M. Hoff (hoff8), N. D. Scielzo (scielzo1)

FS-LDRD-011

Project overview

The Facility for Rare Isotopes Beams (FRIB) will be the flagship facility in low-energy nuclear physics when it comes online in 2022. The β-decay properties of neutron-rich isotopes will be measured with the FRIB Decay Station, a sophisticated state-of-the-art modular multi-detector system envisioned to perform β, γ, n, and charged-particle spectroscopy. In this feasibility study, we used nuclear decay data collected with the FRIB Decay Station precursor, the Beta-Counting Station, currently used at Michigan State University with a radioactive beam produced at the National Superconducting Cyclotron Laboratory to identify the FRIB Decay Station capabilities for future measurements of neutron-rich exotic nuclei at FRIB to help provide a path forward for future measurements of interest to the lab's mission.

Mission impact

The FRIB Decay station will provide a new and unique capability enabling access to numerous radioisotopes in unprecedented quantities and at higher purities than previously available. With this system, decay data on short-lived neutron and proton-rich isotopes as well as their decaying isobars will be available for high-priority measurements of interest to the community and to the Lab. As a result, measurements of decay properties such as half-lives or gamma-ray transition intensities of radioisotopes important to national security needs will be feasible in the coming years. Generating a shortlist of priority measurements important to national security needs is the next priority.